Microchimica Acta
https://doi.org/10.1007/s00604-018-2958-4

ORIGINAL PAPER

Impedimetric gene assay for BCR/ABL transcripts in plasmids of patients with chronic myeloid leukemia

Karen Yasmim Pereira dos Santos Avelino [1] · Isaac Aarón Morales Frías [2] · Norma Lucena-Silva [3,4] · César Augusto Souza de Andrade [1,2] · Maria Danielly Lima de Oliveira [1,2,5]

Received: 6 May 2018 / Accepted: 10 August 2018

Abstract

A label-free impedimetric biosensor was developed for determination of BCR/ABL transcripts. Specific DNA primers were covalently immobilized on a gold electrode modified with carboxylated multiwalled carbon nanotubes (cMWCNTs) and zinc oxide nanoparticles (ZnO-NPs). Aggregation of the ZnO-NPs is prevented by the introduction of an amino-modified silica coating, which also allows a subsequent covalent linkage to cMWCNTs. The impedimetric biosensor was typically operated at a working voltage of +10 mV vs. Ag/AgCl, in a frequency range from 100 mHz to 100 kHz. Studies on the surface morphology and electrochemical properties of the electrode demonstrated improved bioactivity. Amperometric currents and impedimetric parameters, such as charge transfer resistance, varied significantly throughout the construction of the biosensor. The hybridization process was also evidenced by changes in the topography of the surface after exposure to samples containing BCR/ABL. The gene sensor has a linear concentration range for the target gene of 6.94 aM to 694 fM with a limit of detection as low as 0.039 aM. Also, the biosensor is selective and reproducible with a standard deviation of 4.1%. Three replicates for each experimental condition were used. Hence, it is perceived to be a viable tool for early-stage diagnosis of the BCR/ABL fusion gene and monitoring of major molecular remission in clinical samples.

Keywords Biosensor · Carbon nanotubes · Cyclic voltammetry · Electrochemistry · Impedance spectroscopy · Major molecular remission · Zinc oxide

Introduction

The monitoring of major molecular response (MMR) is one of the most important medical intervention for chronic myeloid leukemia (CML) and is essential to assess the patient's response to treatment and for therapeutic decision-making against cancer [1]. BCR (breakpoint cluster region) /ABL (Abelson murine leukemia) fusion gene, also known as Philadelphia chromosome, is an excellent molecular biomarker which accurate diagnosis is crucial to evaluate MMR in CML and reasonably, in acute lymphoid leukemia (ALL) as well. Your presence is prevalent in all cases of CML (accounting for about 20% of adult cases of leukemia [2]), an around 20% of cases of ALL (accounting for about 85% of childhood cases [3]).

Antibody-based methods have some drawbacks since their presence is ubiquitous on both leukemia and normal cells. Thereupon, polymerase chain reaction (PCR)-based diagnoses are preferred for they provide characterization, identification, and data of the percentage of transcripts found in the sample. Moreover, they offer an analytical sensitivity 10^2–10^3 times higher in comparison to cytogenetic testing [4]. Essential disadvantages such as limited protocol adaptation, high costs associated with complex equipment, need for specialized personnel and time-consuming experimental

Electronic supplementary material The online version of this article (https://doi.org/10.1007/s00604-018-2958-4) contains supplementary material, which is available to authorized users.

✉ Maria Danielly Lima de Oliveira
m_danielly@yahoo.com.br

[1] Programa de Pós-Graduação em Bioquímica e Fisiologia, Universidade Federal de Pernambuco, Recife, PE 50670-901, Brazil

[2] Programa de Pós-Graduação em Inovação Terapêutica, Universidade Federal de Pernambuco, Recife, PE 50670-901, Brazil

[3] Fundação Oswaldo Cruz (Fiocruz), Instituto Aggeu Magalhães, Recife, PE 50670-420, Brazil

[4] Laboratório de Biologia Molecular, Departamento de Oncologia Pediátrica, Instituto de Medicina Integral Professor Fernando Figueira (IMIP), Recife, PE 50070-550, Brazil

[5] Departamento de Bioquímica, UFPE, Recife, PE 50670-901, Brazil

Published online: 16 August 2018

protocols are still obstacles to broad implementation of these methodologies.

Electronic biosensing methods such as electrochemical genosensors strategize over the analytical sensibility of the transduction method and the specificity and complementarity of DNA probes. These methods face challenges such as preserving the bioactivity of the immobilized molecules and improving the sensitivity of the transducing surfaces, yet still once prepared, their use is straightforward and effortless [5].

Constructing devices based on inert and nanostructured materials with a high analytical performance that can induce computable changes in the electrochemical response to arising as an innovative alternative. cMWCNTs are exceptional for this purpose since their hexagonal network of sp^2–hybridized carbon atoms are highly disrupted by functional oxidized defects. Also, its intrinsic properties such as high surface-to-volume ratio and conductivity remain available for mediation of electron transfer and amplification of the electric response.

In a like manner, zinc oxide is a semiconducting material whose electronic and physical properties (optical, magnetic, antibacterial and semiconducting) can be adjusted by surface modification and tuning of its isoelectric point (pH 8–10.3). ZnO-NPs also exhibit a high ratio between surface area and volume, catalytic properties and unique optical properties. However, agglomeration is still a drawback for their use in modifications [6]. Reports show diverse methods for chemical functionalization of ZnO-NPs [7, 8]. The self-assembly of silanes over its surface is promising for the development of ordered nanostructured platforms since it retains the intrinsic properties of the metallic oxide and the chemical characteristics of the coating. Through the surface modification, it is possible to obtain improvement of the non-leaching processes, stability and immobilization density.

From the use of cysteine (Cys), cMWCNTs and ZnO-NPs functionalized with 3-Aminopropyl triethoxy silane (APTES), ZnO-NP/NH_2; the authors present a new impedimetric biodevice. The specific choice of these materials allowed to obtain a chemically modified nanostructured platform with free functional groups, ensuring a stable covalent bonding with biomolecules. According to previous studies, this binding mechanism based on multivalency is capable of increasing the uptake of the analyte in orders of magnitude [9]. Through chemical anchoring of a DNA probe on the Cys-cMWCNT-ZnO-NP/NH_2 nanostructured platform was possible to construct a selective and sensitive biosensor for BCR/ABL fusion gene. Furthermore, major molecular remission was studied over cDNA samples obtained from patients previously diagnosed with chronic myeloid leukemia. Lastly, to test the specificity of the biosensor, some of those cDNA samples were artificially contaminated with the DNA of some common infecting pathogens.

Materials and methods

Materials

Cysteine, carboxyl MWCNTs, ZnO-NPs (< 50 nm particle size and a purity >97%), N-hydroxysuccinimide (NHS), N-(3-Dimethylaminopropyl)-N′-ethylcarbodiimide (EDC), APTES and bovine serum albumin (BSA) were purchased from Sigma Aldrich (St. Louis, MO, USA) (https://www.sigmaaldrich.com). Potassium ferricyanide ($K_3[Fe(CN)_6]$), potassium ferrocyanide ($K_4[Fe(CN)_6]$), nitric acid (HNO_3), glutaraldehyde, methanol, acetone and 0.05 μm alumina paste (α-Al_2O_3) were obtained from Vetec Fine Chemistry Ltd. (https://www.sigmaaldrich.com/us-export/vetec-quimica.html). Trizol was obtained from Invitrogen (https://www.thermofisher.com/br/en/home/brands/invitrogen.html).

A recombinant plasmid containing the chimeric gene were obtained according to the methodology described by Marques et al. [10]. Briefly, the BCR/ABL fusion gene was amplified using both ALL (9;22) 5'-NH_2-AGATACTCAGCGGC ATTG-3′ and CML (9;22) primers 5'-AGCTTCTC CCTGACATCCGTG-3′. Subsequently, a pTA vector was used for subcloning of the chimerical DNA fragment. All plasmid samples were validated by conventional PCR (standard technique) and ethidium bromide-stained agarose gel electrophoresis. Thus, the quality of the analytical results of the DNA biosensor was assured.

Complementary DNA (cDNA) samples were obtained from patients of the Pediatric Oncology Service biorepository at the Integral Medicine Institute *Prof. Fernando Figueira*. The clinical samples were collected under the consent of the patients, and the procedures were approved by the local ethics committee. Firstly, bone marrow samples were collected by aspiration from the iliac bone of consecutive and unselected patients for leukemia diagnosis. Then an aliquot of each sample was submitted to molecular biology studies. RNA was extracted from 5×10^6 cells using Trizol, and a random primer was used to perform the reverse transcription of the total RNA into cDNA [10]. Samples were prepared in 10 mM phosphate-buffered saline (PBS) at pH 7.4 and stored frozen. PBS was prepared by adding 10 mM monobasic sodium phosphate to 10 mM dibasic sodium phosphate until a pH of 7.4 is reached [11]. All aqueous solutions were prepared with deionized water obtained from a Milli-Q plus purification system (Billerica, MA, USA).

Chemical modification of ZnO-NPs

APTES-modified ZnO-NPs were obtained as follows. ZnO-NPs (1.5 g) was dispersed into 50 mL of deionized water adjusted to pH = 6.5 with the addition of a HNO_3 solution (2 M) and set in an ultrasonic bath for 10 min to obtain a homogeneous mixture. Then, 1 mL of APTES was added

and set to stirring for further 24 h. Afterward, excess APTES was removed by rinsing with alcohol and acetone three times each. The filtered powder was dried at 60 °C and later stored at room temperature. Before use, ZnO-NP/NH_2 (1 mg.mL^{-1}) was resuspended in methanol, and set in an ultrasonic bath for 5 min to obtain a homogeneous mixture [12]. Functionalization was confirmed by FTIR characterization (Fourier-transform infrared spectroscopy) and the size of the crystallite was assessed by X-ray diffraction (XRD); the results are presented in the supplementary information (Fig. S1 and S2).

Preparation of the transducer

A bare gold electrode (BGE, ϕ= 2 mm) was polished with 0.05 μm α-Al_2O_3 paste, rinsed with deionized water and set in an ultrasonic bath for 10 min. Subsequently, the electrode was electrochemically pretreated; cyclic voltammetry (CV) scanning was performed between −0.2 V and 0.7 in H_2SO_4 (0.5 M) until a typical clean gold CV curve was obtained. Bottom-up construction on the BGE started by dropping 2 μL of a Cys solution (40 mM) prepared in PBS (pH = 7.4) and let to incubate for 30 min to obtain a self-assembled layer. Surface saturation was optimized by studying the electrochemical response of different concentrations of Cys solution (10, 20, 30, 40, 50 and 60 mM) and its results are presented in the supplementary information (Fig.S4a and Fig.S4b). For cMWCNTs immobilization, 4 μg.mL^{-1} were dispersed in methanol and set in an ultrasonic bath for 5 min to obtain a homogeneous mixture. 0.4 M EDC/0.1 M NHS was then introduced to the cMWCNTs suspension at a ratio of 1:1:2 (*v*/v) and let to incubate for 10 min resulting in activated carboxyl groups thus enabling the covalent reaction with cysteine's amino groups. Once activated, 2 μL of the cMWCNTs/EDC: NHS suspension were dropped over the BGE/Cys electrode and then incubated for 20 min. Conjugation was optimized by evaluating the electrochemical response at different incubation times (15, 20, 25, 30 and 35 min) and its results are presented in the supplementary information (Fig.S5). To continue with the construction, the cMWCNTs layer was further activated with 2 μL EDC/NHS 1:1 (*v*/v). Passed 10 min, 2 μL of ZnO-NP/NH_2 suspension (1 mg.mL^{-1}) were added, and the electrode was let to incubate for 20 min. Immobilization of ZnO-NP/NH_2 was optimized by evaluating different incubation times (10, 20, 30, 40, 50 and 60 min) and its results are presented in the supplementary information (Fig.S6). Probe conjugation was developed by dropping 1 μL of glutaraldehyde (16%) over the cMWCNT-ZnO-NP/NH_2 modified electrode and let to incubate for 5 min. To grant selectivity, 1 μL of a 1:1 (*v*/v) mixture of CML and ALL aminated DNA probes (25 pmol.μL^{-1}) was dropped over the cMWCNT-ZnO-NP/NH_2 modified electrode and incubated for 15 min. Finally, the modified electrode was blocked from any nonspecific binding sites by immersing it in a BSA solution (25 pmol.μL^{-1}). The construction of the platform Cys-cMWCNT-ZnO-NP/NH_2-probe-BSA sensor is schematized in Fig. 1.

Evaluation of bioactivity and monitoring of major molecular remission

Initially, the biological samples were heated to 94 °C for DNA denaturation. All assays were performed over a 2 μL sample which was dropped on the biosensor surface and let to incubate for 15 min before reading the electrochemical response. Sensitivity and selectivity were evaluated by studying the electrochemical response of the biosensor after exposure to BCR/ABL-positive and BCR/ABL-negative recombinant plasmids. The responses are considered standard since the molecular weight of each plasmid sample (positive or negative) remains constant. Afterward, bioactivity was evaluated by testing leukemia-positive cDNA samples. Selectivity and specificity were evaluated by testing non-leukemic cDNA samples that contained infecting alien genomes such as *Escherichia coli*, *Candida albicans*, *Mycobacterium tuberculosis*, *Schistosoma mansoni* and Hepatitis C virus (HCV). For determination of major molecular remission, cDNA samples of leukemia-positive patients before and after receiving treatment were tested.

Electrochemical measurements

Electrochemical experiments were performed on a PGSTAT 128 N potentiostat/galvanostat interfaced with NOVA 1.11 software (Metrohm Autolab Inc., Netherlands). The electrochemical cell set in a three-electrode configuration using 10 mM K_3[Fe (CN)$_6$]/K_4[Fe (CN)$_6$] (1:1, *v*/v) in PBS (10 mM, pH 7.4) as redox probe. The cMWCNT-ZnO-NP/NH_2 modified gold electrode was the working electrode. A platinum wire and Ag/AgCl electrode saturated with KCl (3 M) were used as counter and reference electrodes, respectively. CV measurements were carried out at a 50 mV.s^{-1} scan rate in a range of potential between −0.2 V and + 0.7 V. The impedance measurements were recorded in the form of Nyquist plots in a frequency range from 100 mHz to 100 kHz under an AC voltage amplitude of 10 mV. The electrochemical experiments were performed in triplicate at room temperature inside a Faraday cage.

Atomic force microscopy measurements

Topographic characterization was performed using an SPM-9500 atomic force microscope (Shimadzu, Tokyo, Japan). Atomic force microscopy (AFM) images were obtained in noncontact mode with an aluminum-coated silicon cantilever (Multi 75AL, NCHR, resonant frequency = 75 kHz, force constant = 3 N.m^{-1}) at room temperature. Lateral resolution

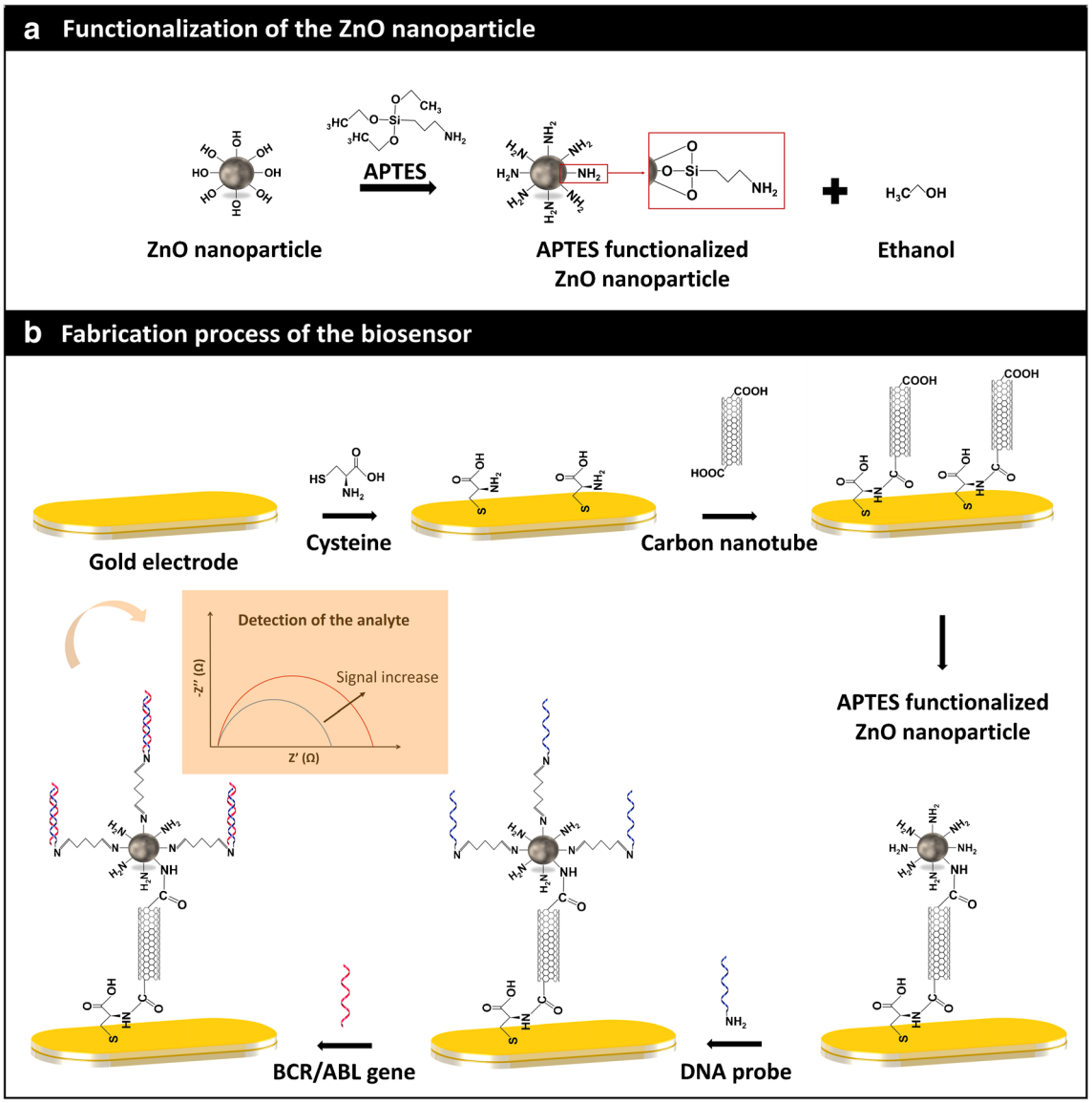

Fig. 1 Representation of the ZnO nanoparticle functionalized with 3-(aminopropyl) triethoxysilane (APTES) (**a**). The combination of cysteine, carbon nanotube, APTES functionalized ZnO nanoparticle and DNA probes were used to engineer a biosensing platform for detection of the BCR/ABL fusion gene (**b**)

was set to 512 × 512 pixels in a scan area of 5 × 5 μm. The images were obtained from at least three macroscopically separated areas of each sample for removal of artifacts. AFM Gwyddion software was used to analyze the images.

Results and discussion

Topographical analyses

3D and 2D AFM images of the biosensor are shown in Fig. 2. The sensitive system based on Cys-cMWCNT-ZnO-NP/NH_2-probe-BSA presents a maximum height of 147 nm (Fig. 2a). In sequence (Fig. 2b), the biosensor was exposed to a leukemia-positive cDNA sample. One observes a drastic change in the height of the sensor system up to 181 nm; this phenomenon is due to the hybridization process between the DNA probe and BCR/ABL transcript expressed in patients with CML. In contrast, non-significant differences in morphology or height were observed after testing a non-leukemic sample (maximum height of 151 nm) (Fig. 2c). Therefore, AFM results suggest the high selectivity of the sensing device. Complementary images related to each stage of assembly of the nanostructured platform are present in Fig. S3.

Electrochemical characterization during biosensor assembly

Figure 3a shows the cyclic voltammograms and impedance spectra (b) for each step of the biosensor assembly. The

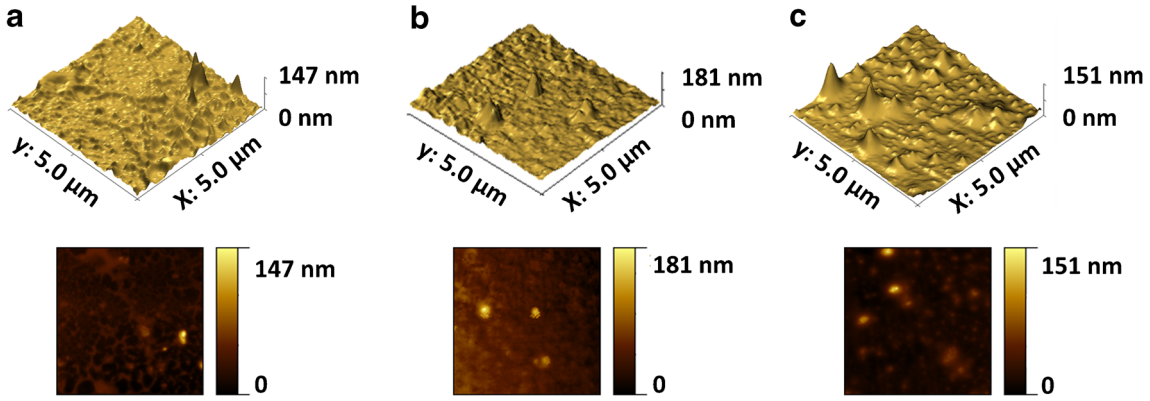

Fig. 2 3D e 2D AFM images for the electrode modified with Cys-cMWCNT-ZnO-NP/NH_2-probe-BSA (**a**), Cys-cMWCNT-ZnO-NP/NH_2-probe-BSA-CML positive sample (**b**) and Cys-cMWCNT-ZnO-NP/NH_2-probe-BSA-CML negative sample (**c**). Scan area of 5 µm × 5 µm

impedimetric responses were fitted using a theoretical simulation of the experimental data through NOVA 1.11 software in the form of a Randle's equivalent circuit (inset of Fig. 3b). Composing the electric circuit, were found the ohmic resistance of the electrolyte solution (Rs) and a Warburg impedance (Z_W) related to mass transport of the electroactive species in the bulk solution to the electrode surface. Accumulation close to the surface of the biosensor is represented by a constant phase element (CPE) and charge transfer resistance (R_{CT}). The values of the equivalent circuit elements obtained from the fitting of the impedance results are shown in the supplementary information (Table S1). As can be observed in Fig. 3a, BGE presents symmetrical and well-defined anodic and cathodic peaks. Its impedimetric spectrum (Fig. 3b) is characterized by an almost linear response that presents a low R_{CT} value (R_{CT} = 0.17 kΩ), this behavior can be associated to electron transfer kinetics in the double electric layer that is mainly controlled by mass diffusion.

Cys is a small thiolated (SH- groups) molecule that interacts strongly with gold atoms using covalent bonds, though multiple layer stacks are considered a strongly physisorbed layer. Cysteine self-assembled layers present a high degree of molecular organization and act as an efficient spacer for the motility of the redox probe, essential features for the development of nanostructured sensors [13]. After modification with Cys, a reduction of the amperometric current (Fig. 3a) and increase in the resistive properties (R_{CT} = 3.36 kΩ) (Fig. 3b) indicate the formation of the Cys layer on the solid substrate. The increase in the resistance is caused by the repulsion of the $[Fe(CN)_6]^{3-}$/ $[Fe(CN)_6]^{4-}$ ions by the carboxyl groups of the Cys molecules, thus altering the charge transfer kinetics in the double electric layer [14]. In this manner, after the immobilization of the nanomaterials, the permeation processes of the redox probe are enhanced. After cMWCNTs are immobilized over the Cys layer, one observes a bigger CV response (Fig. 3a) towards the $[Fe(CN)_6]^{3-}$/$[Fe(CN)_6]^{4-}$ redox couple and a decrease in the impedimetric spectra (R_{CT} = 0.02 kΩ) (Fig. 3b). Despite the obstruction exerted by the cMWCNTs on the electrode surface, it should be noted that MWCNTs are nanomaterials that present high conductivity, which justifies the reduced value of R_{CT} and the increase in the electron transfer rate. Of note, the relatively high electrical conductivity, electrochemical stability and chemical inertness of the cMWCNTs contribute to obtaining sensitive and effective detection systems.

The immobilization of ZnO-NP/NH_2 over the cMWCNT-Cys-modified electrode resulted in a decrease in the amperometric response (Fig. 3a) and an increase in the R_{CT} (2.54 kΩ) (Fig. 3b). Although ZnO is a semiconductor and often increases the charge flow at the electrode/solution interface,

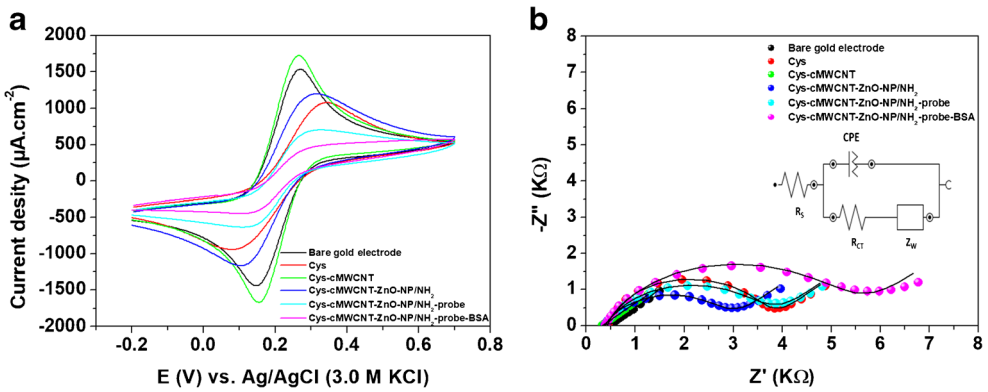

Fig. 3 Cyclic voltammograms (**a**) and impedance spectra (**b**) for each step of assembly of the biosensor. Inset: Equivalent circuit used to fit the impedance measurements

when compared to carbon nanomaterials in previous reports, this electrochemical response has been associated to their insulating nature [15]. At the nano level, ZnO-NPs' surface is highly conductive due to a great density of electrons supplied by H^+ donors, and for the most probable, the APTES surface modification alters this physicochemical behavior. Additionally, the conductivity of the ZnO-NPs is often affected by the presence of oxygen vacancies or interstitial metallic zinc [16]. It is emphasized that the incorporation of ZnO-NP/NH_2 into nanostructured platforms provides functional amino groups for multivalent anchoring of biomolecules. Therefore, this nanomaterial contributes significantly to an effective biorecognition process.

After probe immobilization, a significant decrease in the oxidation/reduction peaks (Fig. 3a) and an increase in the R_{CT} response (Fig. 3b) of the Cys-cMWCNT-ZnO-NP/NH_2 nanostructured surface were observed. This behavior indicates low penetration of the redox probe in the sensor system. Similarly to the effect found on the cMWCNT, some reports appoint that the factors that contribute to this event are the electrostatic repulsion between phosphate groups of the DNA probe and negatively charged polyelectrolytes ($[Fe(CN)_6]^{-3}$ and $[Fe(CN)_6]^{-4}$) [17]. This effect is demonstrated by the current reduction (Fig. 3a) and increase in the impedimetric response ($R_{CT} = 5.08$ kΩ) (Fig. 3b). Finally, BSA was used to prevent unspecific binding and its use results in an increase in the impedimetric response ($R_{CT} = 5.08$ kΩ).

Study of sensitivity and selectivity in plasmid samples assays

Bio-detection sensitivity was studied for concentrations of complementary plasmids ranging from the atto to the femtomolar range (6.94 aM, 694 aM, 6.94 fM, 69.4 fM and 694 fM), and the resultant cyclic voltammograms are shown in Fig. 4a. The decrease in the oxidation/reduction currents reveals the formation of the double-stranded DNA (dsDNA) on the biosensor surface. dsDNA acts as an additional blockade for the passage of the redox probe ions [18] and is expressed by the deviation percentage of the anodic current variation (ΔI) [19].

$$\Delta I(\%) = \left|\frac{I_b - I_a}{I_b}\right| \times 100 \quad (1)$$

Where I_b and I_a correspond to the anodic peak current before and after the hybridization process, respectively. The exposure to BCR/ABL-negative plasmids at a concentration of 694 fM resulted in negligible changes of about $\Delta I = 2.46\%$. This value is lower than that obtained for the minimum positive concentration tested (6.94 aM) $\Delta I = 21.89\%$ (Table S2), therefore suggesting that the biosensor is very much likely to be highly selective.

Reproducibility and standard experimental deviation were assessed as the result of three replicates performed for each sample. Sensitivity was evaluated by creating a calibration plot from the electrochemical impedance spectroscopy (EIS) responses resulting from the exposure of the genosensor to the BCR/ABL fusion gene present in recombinant plasmids. After testing, one notes an increase in diameter of the Nyquist semicircles (Fig. 4b). The analysis of this behavior shows that capturing the plasmids causes a blockage to the charge transfer on the electrode surface. R_{CT} component is best suited to monitor this phenomenon because of the non-conductive properties that distinguish DNA complexes. From the above exposed, to characterize the analytical performance of the biosensor was used the relative variation of the R_{CT} (ΔR_{CT}) as follows.

$$\Delta R_{CT}\ (\%) = \left|\frac{R_{CT(\text{Biosensor}-\text{target DNA})} - R_{CT(\text{Biosensor})}}{R_{CT(\text{Biosensor})}}\right| \times 100 \quad (2)$$

Here, $R_{CT(\text{Biosensor-target DNA})}$ is the measured value after DNA recognition, and $R_{CT(\text{Biosensor})}$ corresponds to the response of the biosensor before recognition (Cys-cMWCNT-ZnO-NP/NH_2-probe-BSA) (Table S1). The calibration test results were best fitted to linear regression (see inset of Fig. 4b) expressed as $y = 16.14 \ln(x) - 17.87$ with a coefficient of determination

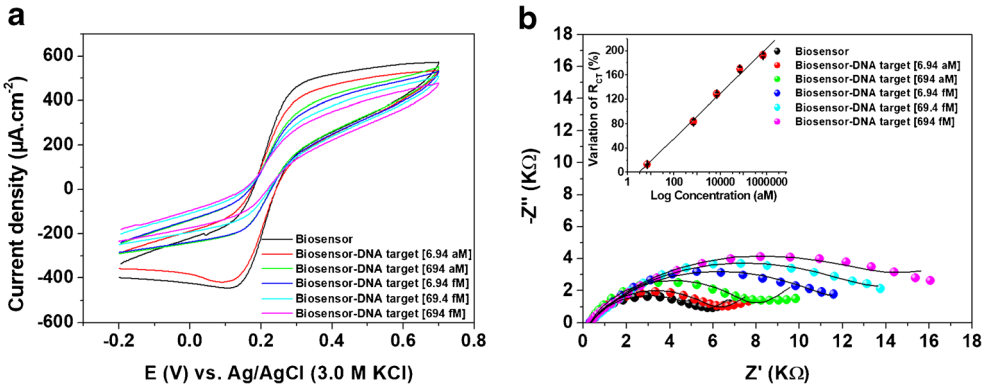

Fig. 4 Cyclic voltammograms (**a**) and impedance spectra (**b**) for the biosensor exposed to different concentrations of recombinant plasmids containing the BCR/ABL fusion gene (DNA target – 6.94 aM, 694 aM, 6.94 fM, 69.4 fM and 694 fM). Inset: Calibration plot of the biosensor. Three replicates for each experimental condition were used. The experimental values are described as the mean values ± their half-deviation

Table 1 Analytical comparison between the biosensor presented in this work and the other DNA biosensors reported in the literature for the electrochemical detection of the BCR/ABL fusion gene

Biosensitive nanostructured platform	Technique	Detection time	Detection limit (M)	Reference
Gold surface – Cys – cMWCNT – ZnONp/NH_2 – aminated DNA probe	CV and EIS	15 min	6.94×10^{-18}	This work
Gold surface – a hybrid composite of gold nanoparticles (AuNps) and polyaniline (PANI) – DNA probe	CV and EIS	15 min	69.40×10^{-18}	[21]
Gold surface – thiolated DNA probe (were used amplification probes and CdSeTe/CdS quantum dots tagging)	ASV	~ 18.5 h	2×10^{-15}	[22]
Carbon paste surface – FePt nanoparticle-decorated electrochemically reduced graphene oxide – DNA probe	EIS	–	2.60×10^{-15}	[23]
ITO coated glass substrate – tri-n-octylphosphine oxide-capped cadmium selenide quantum dots – thiolated DNA probe	DPV	2 min	10×10^{-15}	[24]
Gold surface – thiolated DNA probe (reporter probe labeled biotin)	CV and EIS	60 min	10×10^{-15}	[25]
Glassy carbon surface – poly-eriochrome black T film – AuNps – DNA probe (thiolated hairpin locked nucleic acids)	CV, EIS, and DPV	~ 60 min	1×10^{-13}	[26]
Glassy carbon surface – chitosan – cerium dioxide nanoparticles –MWCNT – AuNps – thiolated DNA probe	CV and DPV	55 min	5×10^{-13}	[27]
Glassy carbon surface – aminobenzene sulfonic acid – aminated DNA probe (18-per locked nucleic acids)	CV, EIS, and DPV	~ 35 min	9.40×10^{-13}	[28]

ASV – anodic stripping voltammetry; CV – cyclic voltammetry; DPV – differential pulse voltammetry; EIS – electrochemical impedance spectroscopy

(R^2) of 0.99, with a limit of detection (LOD) of 0.039 aM and an SD of 4.13%. The LOD was calculated using the formula 3α/slope [20] where α represents the standard deviation of the biodevice and slope is obtained from the linear calibration plot.

The comparison between the biosensor and other DNA biosensors reported in the literature for electrochemical BCR/ABL fusion gene detection is shown in Table 1. Briefly, to the best of our knowledge the sensitivity of the present biosensor excels from those more recent by order of magnitude.

Specificity and monitoring of major molecular remission in leukemia-positive cDNA samples

The specificity of this biosensing system was evaluated with non-leukemic cDNA samples containing the genome of one of the following external infecting agents (XcDNA). XcDNA: hepatitis C virus (HCV), *Candida albicans*, *Mycobacterium tuberculosis*, *Staphylococcus mansoni* and *Escherichia coli*. In Fig. 5a one observes that the magnitude of the electrochemical responses after the bio-detection assay are very much alike to that of the pristine sensor. The ΔR_{CT} analysis (inset in the Fig. 5a) helps to visualize the huge difference in response found between cDNA samples (range from 2.75 to 16.92%) and an actual leukemia-positive sample (around 200%). It appears that the genome of different species does not interfere in the bioanalytical performance of the immobilized probes, therefore suggesting high specificity, at least when the tested infecting agents may be present.

Major molecular remission was evaluated in 10 CML-positive patients. The responses of the initial samples are presented on the left side of Fig. 5b (black bars), and the responses obtained after treatment are presented on the right side

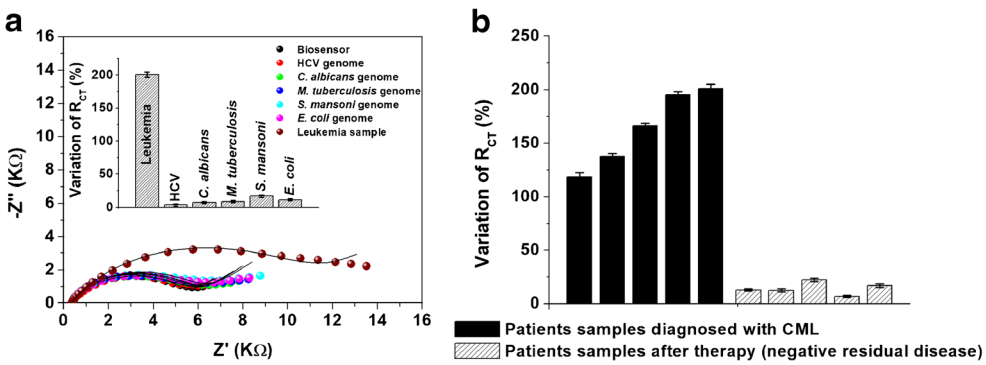

Fig. 5 Impedimetric response for the study with cDNA sample of leukemia patient and cDNA samples of non-leukemic patients containing the genome of HCV, *C. albicans*, *M. tuberculosis*, *S. mansoni* and *E. coli* (**a**). Inset: ΔR_{CT} (%) values obtained from the assays with positive leukemia sample and negative leukemia samples containing the genome of different species. ΔR_{CT} values for the bio-detection assay with cDNA samples of different leukemia patients (**b**). Three replicates for each experimental condition were used; experimental values are described as the mean values ± their half-deviation

(white bars). Is easy to identify two different profiles of electrochemical response characterized by ΔR_{CT}. Patients' samples initially diagnosed with CML result in ΔR_{CT} values varying from 118.50 to 201.18%. After treatment, the same patients seize and expressive reduction of the impedimetric response (ranging from 6.69 to 22.24%), which according to our sensitivity studies accounts for a reduction from around 500 fM to 5 aM (three orders of magnitude).

Cys-cMWCNT-ZnO-NP/NH_2-probe-BSA biosensor can be exhibit some disadvantages. Of note, the stability of the biosystem depends on the natural properties of the molecule that can be denaturated under environmental conditions (pH, temperature or ions). In addition, special attention should be given to the storage conditions and the long-term stability of the biosensor to ensure receptor bioactivity (DNA probe).

Conclusions

The covalent synergy of elite nanomaterials, as for the first time, amino-functionalized silane-coated ZnO and carboxyl MWCNTs was explored and used to engineer a bottom-up chronic myeloid leukemia biosensing platform. Covalent bonding strategy (starting with a Cys self-assembled layer on gold) allowed the construction of a nanostructured non-leeching selective device with ultra-high sensitivity at the attomolar range. Compared with other leukemia biosensors, the present biosensor excels in sensitivity by ten times [19], and its robust characteristics appoint the possibility to help in the development of point of care diagnostics. Therefore, the biosensor can be considered a valuable resource for the clinical research of the BCR/ABL fusion gene, contributing to the early diagnosis of cancer and the monitoring of major molecular remission. The nanostructured platform can be used in the development of biosensors for different purposes such as medical diagnostic, food quality control, environmental monitoring, defense, and pharmaceutical industry. However, some obstacles such as the portability and miniaturization of the sensor system need to be overcome to become viable for commercial application.

Acknowledgments This work was supported by the Brazilian National Council for Scientific and Technological Development/CNPq [grant numbers 302885/2015-3, 310364/2015-9 and 302930/2015-9]; the Brazilian Health Ministry Project DECIT-FINEP-CNPq [grant numbers 1299/2013 and 401700/2015-1]; and the FACEPE-PPSUS-APQ [grant number 0040-4.00/13]. Isaac A. M. Frias would like to thank CAPES and FACEPE for a postdoctoral fellowship and Karen Y. P. S. Avelino would like to thank CNPq for the master scholarship.

Compliance with ethical standards All procedures followed were in accordance with the ethical standards.

References

1. Sung PJ, Luger SM (2017) Minimal residual disease in acute myeloid leukemia. Curr Treat Options in Oncol 18(1):1. https://doi.org/10.1007/s11864-017-0447-3
2. Arrigoni E, Del Re M, Galimberti S, Restante G, Rofi E, Crucitta S, Baratè C, Petrini M, Danesi R, Di Paolo A (2018) Concise review: chronic myeloid leukemia: stem cell niche and response to pharmacologic treatment. Stem Cells Transl Med 7(3):305–314
3. Jyotsana N, Sharma A, Chaturvedi A, Scherr M, Kuchenbauer F, Sajti L, Barchanski A, Lindner R, Noyan F, Sühs KW, Grote-Koska D, Brand K, Vornlocher HP, Stanulla M, Bornhauser B, Bourquin JP, Eder M, Thol F, Ganser A, Humphries RK, Ramsay E, Cullis P, Heuser M (2017) RNA interference efficiently targets human leukemia driven by a fusion oncogene in vivo. Leukemia 32:224–226. https://doi.org/10.1038/leu.2017.269 https://www.nature.com/articles/leu2017269#supplementary-information
4. Vinhas R, Cordeiro M, Pedrosa P, Fernandes AR, Baptista PV (2017) Current trends in molecular diagnostics of chronic myeloid leukemia. Leuk Lymphoma 58(8):1791–1804. https://doi.org/10.1080/10428194.2016.1265116
5. Frias IAM, Avelino KYPS, Silva RR, Andrade CAS, Oliveira MDL (2015) Trends in biosensors for HPV: identification and diagnosis. Journal of Sensors 2015:16–16. https://doi.org/10.1155/2015/913640
6. Kumar R, Umar A, Kumar G, Nalwa HS (2017) Antimicrobial properties of ZnO nanomaterials: a review. Ceram Int 43(5):3940–3961. https://doi.org/10.1016/j.ceramint.2016.12.062
7. Hang TTX, Dung NT, Truc TA, Duong NT, Van Truoc B, Vu PG, Hoang T, Thanh DTM, Olivier M-G (2015) Effect of silane modified nano ZnO on UV degradation of polyurethane coatings. Prog Org Coat 79:68–74. https://doi.org/10.1016/j.porgcoat.2014.11.008
8. Rabin Nurun N, Morshed J, Akhter H, Islam Md S, Hossain Md A, Elias M, Alam Md M, Karim MR, Hasnat MA, uddin Md N, Siddiquey Iqbal A (2016) Surface Modification of the ZnO Nanoparticles with γ-Aminopropyltriethoxysilane and Study of Their Photocatalytic Activity, Optical Properties and Antibacterial Activities. International Journal of Chemical Reactor Engineering, vol 14. https://doi.org/10.1515/ijcre-2015-0141
9. Zanghelini F, Frías IAM, Rêgo MJBM, Pitta MGR, Sacilloti M, Oliveira MDL, Andrade CAS (2017) Biosensing breast cancer cells based on a three-dimensional TIO2 nanomembrane transducer. Biosens Bioelectron 92:313–320. https://doi.org/10.1016/j.bios.2016.11.006
10. Marques EALV, Neves L, Fonseca TC, Lins MM, Pedrosa F, Lucena-Silva N (2011) Molecular findings in childhood leukemia in Brazil: high frequency of MLL-ENL fusion/t(11;19) in infant leukemia. J Pediatr Hematol Oncol 33(6):470–474. https://doi.org/10.1097/MPH.0b013e3181fb8f61
11. Weeks ML, Rahman T, Frymier PD, Islam SK, McKnight TE (2008) A reagentless enzymatic amperometric biosensor using vertically aligned carbon nanofibers (VACNF). Sensors Actuators B Chem 133(1):53–59. https://doi.org/10.1016/j.snb.2008.01.060
12. Grasset F, Saito N, Li D, Park D, Sakaguchi I, Ohashi N, Haneda H, Roisnel T, Mornet S, Duguet E (2003) Surface modification of zinc oxide nanoparticles by aminopropyltriethoxysilane. J Alloys Compd 360(1–2):298–311. https://doi.org/10.1016/S0925-8388(03)00371-2
13. Luna DMN, Avelino KYPS, Cordeiro MT, Andrade CAS, Oliveira MDL (2015) Electrochemical immunosensor for dengue virus serotypes based on 4-mercaptobenzoic acid modified gold nanoparticles on self-assembled cysteine monolayers. Sensors Actuators B Chem 220:565–572. https://doi.org/10.1016/j.snb.2015.05.067
14. Costa MP, Frías IAM, Andrade CAS, Oliveira MDL (2017) Impedimetric immunoassay for aflatoxin B1 using a cysteine

modified gold electrode with covalently immobilized carbon nanotubes. Microchim Acta:1–9. https://doi.org/10.1007/s00604-017-2308-y
15. Das M, Sumana G, Nagarajan R, Malhotra BD (2010) Application of nanostructured ZnO films for electrochemical DNA biosensor. Thin Solid Films 519(3):1196–1201. https://doi.org/10.1016/j.tsf.2010.08.069
16. Arya SK, Saha S, Ramirez-Vick JE, Gupta V, Bhansali S, Singh SP (2012) Recent advances in ZnO nanostructures and thin films for biosensor applications: review. Anal Chim Acta 737:1–21. https://doi.org/10.1016/j.aca.2012.05.048
17. Ferapontova EE (2017) Hybridization biosensors relying on electrical properties of nucleic acids. Electroanalysis 29(1):6–13. https://doi.org/10.1002/elan.201600593
18. Ye Y, Gao J, Zhuang H, Zheng H, Sun H, Ye Y, Xu X, Cao X (2017) Electrochemical gene sensor based on a glassy carbon electrode modified with hemin-functionalized reduced graphene oxide and gold nanoparticle-immobilized probe DNA. Microchim Acta 184(1):245–252. https://doi.org/10.1007/s00604-016-1999-9
19. Avelino KYPS, Frias IAM, Lucena-Silva N, Gomes RG, de Melo CP, Oliveira MDL, Andrade CAS (2016) Attomolar electrochemical detection of the BCR/ABL fusion gene based on an amplifying self-signal metal nanoparticle-conducting polymer hybrid composite. Colloids Surf B: Biointerfaces 148:576–584. https://doi.org/10.1016/j.colsurfb.2016.09.029
20. Bala R, Kumar M, Bansal K, Sharma RK, Wangoo N (2016) Ultrasensitive aptamer biosensor for malathion detection based on cationic polymer and gold nanoparticles. Biosens Bioelectron 85:445–449
21. Avelino KY, Frias IA, Lucena-Silva N, Gomes RG, de Melo CP, Oliveira MD, Andrade CA (2016) Attomolar electrochemical detection of the BCR/ABL fusion gene based on an amplifying self-signal metal nanoparticle-conducting polymer hybrid composite. Colloids Surf B: Biointerfaces 148:576–584. https://doi.org/10.1016/j.colsurfb.2016.09.029
22. Hu L, Tan T, Chen G, Zhang K, Zhu J-J (2013) Ultrasensitive electrochemical detection of BCR/ABL fusion gene fragment based on polymerase assisted multiplication coupling with quantum dot tagging. Electrochem Commun 35:104–107. https://doi.org/10.1016/j.elecom.2013.08.004
23. Yang J, Zhang W (2014) Indicator-free impedimetric detection of BCR/ABL fusion gene based on ordered FePt nanoparticle-decorated electrochemically reduced graphene oxide. J Solid State Electrochem 18(10):2863–2868. https://doi.org/10.1007/s10008-014-2551-7
24. Sharma A, Pandey CM, Matharu Z, Soni U, Sapra S, Sumana G, Pandey MK, Chatterjee T, Malhotra BD (2012) Nanopatterned cadmium Selenide Langmuir–Blodgett platform for leukemia detection. Anal Chem 84(7):3082–3089. https://doi.org/10.1021/ac202265a
25. Wang K, Chen J, Chen J, Liu A, Li G, Luo H, Lin X, Chen Y (2009) A sandwich-type electrochemical biosensor for detection of BCR/ABL fusion gene using locked nucleic acids on gold electrode. Electroanalysis 21(10):1159–1166. https://doi.org/10.1002/elan.200804507
26. Lin L, Chen J, Lin Q, Chen W, Chen J, Yao H, Liu A, Lin X, Chen Y (2010) Electrochemical biosensor based on nanogold-modified poly-eriochrome black T film for BCR/ABL fusion gene assay by using hairpin LNA probe. Talanta 80(5):2113–2119. https://doi.org/10.1016/j.talanta.2009.11.017
27. Li S, Wang L, Li Y, Zhu X, Zhong L, Lu L, Zhang W, Liu B, Xie G, Feng W (2013) Electrochemical determination of BCR/ABL fusion gene based on in situ synthesized gold nanoparticles and cerium dioxide nanoparticles. Colloids Surf B: Biointerfaces 112:344–349. https://doi.org/10.1016/j.colsurfb.2013.07.027
28. Chen J, Zhang J, Wang K, Lin X, Huang L, Chen G (2008) Electrochemical biosensor for detection of BCR/ABL fusion gene using locked nucleic acids on 4-Aminobenzenesulfonic acid-modified glassy carbon electrode. Anal Chem 80(21):8028–8034. https://doi.org/10.1021/ac801040e